Joint 3D Trajectory and Power Optimization for UAV-aided mmWave MIMO-NOMA Networks

Wanmei Feng, Nan Zhao, *Senior Member, IEEE*, Shaopeng Ao,
Jie Tang, *Senior Member, IEEE*, Xiuyin Zhang, *Senior Member, IEEE*,
Yuli Fu, Daniel K. C. So and Kai-Kit Wong, *Fellow, IEEE*

Abstract

This paper considers an unmanned aerial vehicle (UAV)-aided millimeter Wave (mmWave) multiple-input-multiple-output (MIMO) non-orthogonal multiple access (NOMA) system, where a UAV serves as a flying base station (BS) to provide wireless access services to a set of Internet of Things (IoT) devices in different clusters. We aim to maximize the downlink sum rate by jointly optimizing the three-dimensional (3D) placement of the UAV, beam pattern and transmit power. To address this problem, we first transform the non-convex problem into a total path loss minimization problem, and hence the optimal 3D placement of the UAV can be achieved via standard convex optimization techniques. Then, the multiobjective evolutionary algorithm based on decomposition (MOEA/D) based algorithm is presented for the shaped-beam pattern synthesis of an antenna array. Finally, by transforming the original problem into an optimal power allocation problem under the fixed 3D placement of the UAV and beam pattern, we derive the closed-form expression of transmit power based on Karush-Kuhn-Tucker (KKT) conditions. In addition, inspired by fraction programming (FP), we propose a FP-based suboptimal algorithm to achieve a near-optimal performance. Numerical results demonstrate that the proposed algorithm achieves a significant performance gain in terms of sum rate for all IoT devices, as compared with orthogonal frequency division multiple access (OFDMA) scheme.

Index Terms

Internet of Things, multi-beam, non-orthogonal multiple access, power allocation, UAV.

I. Introduction

The rapid development of Internet of Things (IoT) paradigm has led to an exponential growth in connected IoT devices and generated data. As a result, the fifth generation (5G) and beyond 5G (B5G) wireless networks are facing significant technical challenges to meet the demands for high-reliability and ulter-high capacity wireless communications [1]. Millimeter wave (mmWave) communications have been considered as one of the potential technologies since it can potentially achieve high aggregate capacity in 5G/B5G networks [2]. In addition, process techniques such as beamforming can concentrate the signal energy from massive multiple-input-multiple-output (MIMO) antenna arrays to overcome the high propagation loss at mmWave frequencies. Therefore, the combination of mmWave and massive MIMO can greatly improve the spectral efficiency (SE) for future 5G/B5G wireless networks [3], [4].

Due to the constraint of hardware architecture and the high cost of radio frequency (RF) chains in mmWave MIMO systems, the number of RF chains is much less than the numbers of antennas, which limites the performance of multi-user mmWave MIMO systems [2]. Therefore, multiple access techniques have been regarded as one of the most fundamental enablers to support massive connectivity requirement in 5G/B5B systems. In particular, there are two types of multiple access schemes for wireless networks, namely, orthogonal multiple access (OMA) technique and non-orthogonal multiple access (NOMA) technique. OMA technique includes time division multiple access (TDMA), orthogonal frequency division multiple access (OFDMA) and code division multiple access (CDMA), which allocates each resource block (time/frequency/code) to at most one user [5]. Since one resource block can only be assigned to a single user, the enhancement in SE is still limited. Compared with OMA scheme, NOMA technique which enables multiple users to share the same physical resources, can achieve better performance in terms of system SE [5]. Hence, NOMA networks have attracted significant attention in the research community and industry [6]–[12]. In [6], an energy-efficient resource allocation strategy was investigated for

maximizing the system energy efficiency (EE) in a downlink NOMA network, where subchannel assignment and power allocation were considered. The authors in [7] studied the secrecy rate maximization problem in a single-input single-output (SISO) NOMA system while guaranteeing quality of service (QoS) requirements, in which the closed-form expressions of optimal power allocation coefficients were derived. A joint user scheduling and power allocation scheme for NOMA-based downlink networks was proposed in [8] to minimize the power consumption of the base station (BS) and wireless mobile devices. An efficient resource allocation algorithm was proposed in [9] to maximize the EE of a downlink NOMA network subject to the minimum rate requirements and the maximum transmission power constraint of users, where subchannel assignment and power allocation were taken into account. Based on the aforementioned works, the application of mmWave MIMO in NOMA systems have attracted great attention recently [10]–[12]. In [10], the authors investigated the closed-form expressions for the ergodic capacity under two different SNR regimes in mmWave MIMO-NOMA systems. In [11], the authors investigated a joint beamforming and power allocation strategy to maximize the minimum achievable data rate in mmWave-NOMA systems with analog beamforming, where a closed-form expression of power allocation was derived and beamforming vectors were obtained. A resource allocation scheme was proposed in [12] for maximizing the overall system performance in multi-beam NOMA systems, wherein the multi-beams were formed by a hybrid mmWave structure.

In fact, when IoT devices located in an area with limited or without infrastructure coverage, it is not efficient to deploy BSs to provide wireless access services. Fortunately, due to advantages of autonomy, flexibility and mobility, unmanned aerial vehicles (UAVs) can enable dynamic deployments and offer cost-effective wireless services for the edge IoT devices, and hence it has been widely adopted in many applications including wireless power transfer (WPT) networks [13], wireless powered communication networks (WPCNs) [14], emerging networks [15], satellite communication systems [16] and solar power systems [17]. Based on the aforementioned works on UAV-aided wireless networks, the application of UAVs in MIMO-NOMA systems have

attracted many research attention recently [18]–[21]. In [18], a machine learning framework was exploited to determine the three-dimensional (3D) placement of UAVs in NOMA-enabled UAV networks, where power allocation and trajectory design were taken into account. In [19], a sum-rate maximization problem was studied in NOMA-UAV networks by jointly optimizing the 2D placement and transmit power of a UAV. To further improve the SE of the system, the application of mmWave MIMO techniques in NOMA-based UAV networks have attracted attention from research communities as well as industry [20], [21]. In [20], a stochastic geometry method was employed to model the locations of users and interference in MIMO-NOMA assisted UAV networks, in which the closed-form expressions for the outage probability and ergodic rate of the system were given. In [21], a beam scanning approach was studied to maximize the achievable sum rates in UAV-aided NOMA networks, and the closed-form expressions of outage probabilities and average sum rate were derived.

A. Main contributions

Previous works in the literature focus on maximizing the system performance in NOMA based wireless networks [6]–[9] and mmWave MIMO-NOMA systems [10]–[12], where UAVs are not considered to extend the wireless coverage of users. On the other hand, the works in [18], [19] aim to investigate the power allocation and deployment optimization for UAVs, but do not take into account mmWave MIMO-NOMA techniques. In addition, the works in [20], [21] focus on studying the outage probability of the sum-rate in MIMO-NOMA enhanced UAV networks without considering the effect of the 3D placement and power allocation of UAVs. In contrast to [6]–[21], in this paper, we investigate the sum-rate maximization problem for UAV-aided mmWave MIMO-NOMA networks, where the 3D location of the UAV, beam pattern and transmit power are jointly considered. Furthermore, both the optimal and suboptimal power allocation schemes are proposed. The main contributions of this paper are summarized as follows.

- We propose a theoretical model for sum-rate maximization in UAV-aided mmWave MIMO-

NOMA networks, where the 3D location of a UAV, beam pattern and transmit power are jointly optimized. To tackle this problem, we decompose the optimization problem into three sub-problems, particular for optimizing the 3D placement of the UAV, beam pattern and transmit power, and solve these three sub-problems sequentially.

- First, the original problem is converted into a total path loss minimization problem, and the optimal altitude can be computed via monotonic optimization theory. Besides, the optimal 2D location of the UAV can be obtained by using standard convex optimization techniques. Then, the multiobjective evolutionary algorithm based on decomposition (MOEA/D) based algorithm is introduced to optimize the beam pattern. Finally, given the optimal 3D position of the UAV and designed beam patterns, the formulated problem is equivalent to a transmit power optimization problem. To tackle this problem, an optimal power allocation scheme is proposed, for which the closed-form expression of power allocation is derived via Karush-Kuhn-Tucker (KKT) conditions. Moreover, a fractional programming (FP)-based suboptimal algorithm is proposed to obtain a near-optimal solution.
- Simulation results show that the proposed algorithm can achieve a significant gain performance in terms of throughput. Moreover, simulation results also verify that the proposed FP-based suboptimal solution performs very close to the optimal power allocation scheme.

B. Organization and Notation

The remainder of this paper is organized as follows. In Section II, the system model is described, and then the sum-rate maximization problem is formulated. In Section III, a joint 3D deployment, beam pattern design and power allocation algorithm is proposed to solve the sum-rate maximization problem. Numerical results are presented in Section IV, and finally, conclusions are provided in Section V.

The following notations are used in this paper. Boldface letters represent vectors. $\mathbf{a}^T$ and $\mathbf{a}^H$ denote the transpose and complex conjugate transpose of the vector $\mathbf{a}$, and $\|\mathbf{a}\|$ represents the

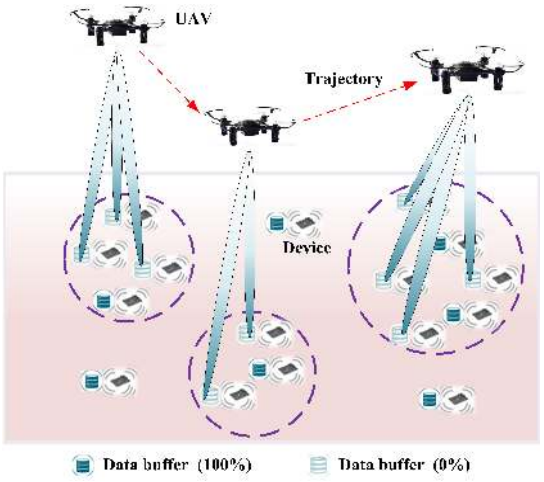

Fig. 1: Illustration of a UAV-aided mmWave MIMO-NOMA network with multi-beams and power allocation.

Euclidean norm. We use $\mathbf{R}$ to denote a set of real numbers, and use $\mathbf{R}_{+}(\mathbf{R}_{++})$ to denote the set of nonnegative (strictly positive) real numbers.

II. System Model and Problem Formulation

A. System model

We consider a downlink mmWave MIMO-NOMA transmission system as shown in Fig. 1, where a rotary-wing UAV flies above the serving areas and disseminates data towards multiple IoT devices simultaneously at each waypoint. The UAV is mounted with an $M \times N$ antenna array, while a single antenna is assumed at each IoT device. In this paper, we adopt an analog beamforming (BF) structure as the multi-beam generation scheme. In particular, the total antenna array elements at the UAV is separated into multiple sub-arrays, wherein the beam direction radiated from each sub-array is controlled by the value of the phase shifters. Moreover, the mutual coupling among sub-arrays is negligible in an analog BF structure whilst the mutual coupling between two elements in a sub-array is taken into account.

We denote the 2D locations of the UAV by $z_u = (x_u, y_u)$, and its altitude as h. The location of the device $k \in \{1, 2, \cdots K\}$ on the ground are $z_k = (x_k, y_k)$. Since UAVs can be flexibly deployed and moved in 3D place, we assume that the UAV-ground channel is line-of-sight

(LoS)-dominated, and the channel $\mathbf{h}_k$ between the UAV and device k is given by [22], [23]

$$\mathbf{h}_k = \sqrt{\beta_0 d_k^{-\alpha}}\mathbf{a}(\theta, \phi), \tag{1}$$

where α ($\alpha \geq 2$) and $d_k = \sqrt{(x_k - x_u)^2 + (y_k - y_u)^2 + h^2}$ are the path loss exponent and the distance between the UAV and the device k, respectively. β_0 denotes the path loss at the reference distance of $d_0 = 1$ m. In addition, let λ and d_{array} be the wavelength and the spacing between antenna elements. The steering vector $\mathbf{a}(\theta, \phi)$ with the elevation θ and azimuth ϕ angles of an $M \times N$ antenna array can be expressed as

$$\begin{aligned}\mathbf{a}(\theta, \phi) =&[1, \cdots, e^{j2\pi/\lambda d_{array}\sin(\theta)[(m-1)\cos(\phi)+(n-1)\sin(\phi)]},\\ &\cdots, e^{j2\pi/\lambda d_{array}\sin(\theta)[(M-1)\cos(\phi)+(N-1)\sin(\phi)]}]^T,\end{aligned} \tag{2}$$

where m and n are the indices of the antenna elements in $x-y$ plane, respectively. Furthermore, let $\mathbf{w}$ be the beamforming vector. The effective channel gain between the UAV and the device k is given as

$$|\mathbf{h}_k^H \mathbf{w}|^2 = \frac{\beta_0}{[(x_k - x_u)^2 + (y_k - y_u)^2 + h^2]^{\alpha/2}}|\mathbf{a}^H(\theta, \phi)\mathbf{w}|^2, \tag{3}$$

where $\mathbf{E}(\theta, \phi) = \mathbf{a}^H(\theta, \phi)\mathbf{w}$ indicates the synthesized pattern of the $M \times N$ antenna array, and $\mathbf{w} = [w_{1n}, \cdots, w_{mn}, \cdots, w_{MN}]^T$. $w_{mn} = p_{mn}(\theta, \phi)I_{mn} \cdot e^{j\beta_{mn}}$ illustrates the amplitude excitation and phase of the (m, n)th array element, where $p_{mn}(\theta, \phi)$ and I_{mn} denote the active pattern and amplitude excitation of the (m, n)th element, respectively. Therefore, the synthesized pattern $\mathbf{E}(\theta, \phi)$ can be equivalently written as [24]

$$\mathbf{E}(\theta, \phi) = \sum_{m=1}^{M}\sum_{n=1}^{N} p_{mn}(\theta, \phi)I_{mn} \times e^{j\psi(\theta,\phi)}, \tag{4}$$

where $\psi(\theta, \phi) = 2\pi/\lambda d_{array}\sin(\theta)[(m-1)\cos(\phi) + (n-1)\sin(\phi)] + \beta_{mn}$, and β_{mn} denotes the progressive phase shift that can be controlled by phase shifters to determine main beam directions. In addition, we define $AF = \sum_{m=1}^{M}\sum_{n=1}^{N} I_{mn} \times e^{j\psi(\theta,\phi)}$ as the array factor of the

$M \times N$ antenna array.

B. Transmit and receive strategy for NOMA system

Consider the case where there are Γ groups to be served by the UAV, and all the devices share the same subcarrier in order to yield significant performance gains [5]. Therefore, the UAV transmits a signal s_k to the device k with the transmit power p_k, and the received signal at this device k is given by

$$y_k = \mathbf{h}_k^H \mathbf{w} \sum_{k=1}^{K} \sqrt{p_k} s_k + n_k, \tag{5}$$

where $n_k \sim \mathcal{CN}(0, \sigma^2)$ represents the additive white Gaussian noise (AWGN) at device k with power σ^2.

According to the NOMA scheme, successive interference cancellation (SIC) is employed to decode users, and the decoding order for NOMA users depends on the effective channel gain $|\mathbf{h}_k^H \mathbf{w}|^2$. However, the decoding order can not be determined before beamforming, and thus we define the decoding order by the channel gains of devices. Without loss of generality, we assume that $\|\mathbf{h}_1\| < \|\mathbf{h}_2\| < \cdots < \|\mathbf{h}_K\|$. Using this assumption, the signal-to-interference-plus-noise-radio (SINR) of the device $k = \{1, 2, \cdots, K-1\}$ can be expressed as

$$SINR_k = \frac{p_k |\mathbf{h}_k^H \mathbf{w}|^2}{\sum_{i=k+1}^{K} p_i |\mathbf{h}_k^H \mathbf{w}|^2 + \sigma^2}. \tag{6}$$

For the Kth device, the SINR is given by

$$SINR_K = \frac{p_K |\mathbf{h}_K^H \mathbf{w}|^2}{\sigma^2}. \tag{7}$$

From (6) and (7), the achievable rate of the device $k = \{1, 2, \cdots, K\}$ is given by

$$R_k = \log_2(1 + SINR_k). \tag{8}$$

C. Problem formulation

In this paper, we formulate the sum rate maximization problem to maximize the sum rate of all IoT devices. Mathematically, this problem is formulated as

$$(\mathrm{P1}): \max_{z_u, h, p_k, \mathbf{E}(\theta,\phi)} \sum_{k=1}^{K} \log_2(1 + SINR_k) \tag{9}$$

$$\text{s.t. } \|z_k - z_u\|^2 \leq h^2 \tan^2 \Theta, \tag{10}$$

$$h_{min} \leq h \leq h_{max}, \tag{11}$$

$$R_k \geq r_k, \tag{12}$$

$$\sum_{k=1}^{K} p_k \leq P_{max}. \tag{13}$$

In constraint (10), 2Θ denotes the effective illumination angle of beams. This constraint guarantees that the horizontal distance between the UAV and IoT devices is less than the coverage radius of the UAV $h \tan \Theta$. Constraint (11) is the boundary constraint for the altitude of UAV. Constraint (12) is imposed such that the transmission rate of device k should be larger than the rate threshold r_k in order to guarantee a minimum data rate for all IoT devices. Constraint (13) denotes the transmission power constraint, in which P_{max} is the total transmission power. The sum-rate maximization problem is mixed combinatorial non-convex. In the following, we propose an effective algorithm to tackle the problem (P1).

III. Joint 3D deployment, beam pattern design and power allocation algorithm

In this section, we propose a joint 3D deployment, beam pattern design and power allocation algorithm where the original problem is decomposed into three sub-problems and the 3D position of the UAV (x_u, y_u, h), beam pattern $\mathbf{E}(\theta, \phi)$ and transmit power p_k are optimized sequentially. Specifically, since the generation of beam pattern needs to acquire the beam scanning angles, the

3D placement of the UAV should be optimized first. Then, based on the angle information of devices, the beam pattern can be designed. Finally, with the optimized 3D placement of the UAV and designed beam patterns, the original problem can be further transformed into an optimization problem with a single variable p_k. Therefore, in our proposed algorithm, we first transform the original problem into a sub-problem of minimizing the total path loss, and the optimal altitude h^* can be obtained by exploiting the monotonicity property of the objective function. Then, the optimal 2D position of the UAV (x_u^*, y_u^*) is obtained via the first-order derivatives of x_u and y_u under a fixed h^*. Subsequently, we propose the MOEA/D based algorithm to design the beam pattern $\mathbf{E}(\theta, \phi)$. Finally, we propose an optimal and a sub-optimal power allocation scheme to optimize the transmit power of the UAV p_k, respectively.

A. Optimal UAV 3D location

For given p_k and $\mathbf{E}(\theta, \phi)$, problem (P1) is formulated as

$$(\text{P2}): \max_{z_u, h} \sum_{k=1}^{K} \log_2(1 + SINR_k) \tag{14}$$

$$\text{s.t. } \|z_k - z_u\|^2 \leq h^2 \tan^2 \Theta, \tag{15}$$

$$h_{min} \leq h \leq h_{max}. \tag{16}$$

Problem (P2) is non-convex due to the non-convexity of the objective function and constraint (15). The path loss model for LoS link between the UAV and the device k is given by [19]

$$L_{LoS}^k = 20 \log_{10}(4\pi f_c d_k / c + \eta_{LoS}), \tag{17}$$

where f_c and c are the carrier frequency and speed of light, respectively. η_{LoS} represents the mean additional loss for LoS transmission. Accordingly, the received power of the device k is given by [19]

$$p_r^k = 10\log_{10} p_k - L_{LoS}^k. \tag{18}$$

From (18), it is observed that the received power of the device k depends on the path-loss exponent. Motivated by this, problem (P2) can be modified to minimize the total path loss subject to flight altitude and wireless coverage radius as

$$(\text{P3}): \min_{L_{LoS}^k} \ \sum_{k=1}^{K} L_{LoS}^k \tag{19}$$

$$\text{s.t. } \|z_k - z_u\|^2 \leq h^2 \tan^2\Theta, \tag{20}$$

$$h_{min} \leq h \leq h_{max}, \tag{21}$$

$$\min\{x_i\} \leq x_u \leq \max\{x_i\}, 1 \leq i \leq K, \tag{22}$$

$$\min\{y_i\} \leq y_u \leq \max\{y_i\}, 1 \leq i \leq K. \tag{23}$$

By substituting (17), problem (P3) can be expressed as problem (P3.1)

$$(\text{P3.1}): \min_{d_k} \ 20\log_{10}\left(\prod_{k=1}^{K}\left(\frac{4\pi f_c d_k}{c}\right)\right) + K\eta_{LoS} \tag{24}$$

$$\text{s.t. } \|z_k - z_u\|^2 \leq h^2 \tan^2\Theta, \tag{25}$$

$$h_{min} \leq h \leq h_{max}, \tag{26}$$

$$\min\{x_i\} \leq x_u \leq \max\{x_i\}, 1 \leq i \leq K, \tag{27}$$

$$\min\{y_i\} \leq y_u \leq \max\{y_i\}, 1 \leq i \leq K. \tag{28}$$

It should be noted that the objection function of problem (P3.1) increases monotonously with the increase of d_k, and d_k is determined by the UAV deployment. As a result, the optimal 3D location of the UAV can be computed by minimizing the total path loss of UAV-ground transmission. Besides, $\prod_{k=1}^{K}(4\pi f_c d_k/c)$ can be rewritten as $(4\pi f_c/c)^K(d_1 d_2 \cdots d_K)$, and $K\eta_{LoS}$ is a constant component of the objective function. Thus, by applying the inequality $d_1 d_2 \cdots d_K \leq ((d_1+d_2+\cdots+d_K)/K)^K$ in [19], problem (P3.1) is equivalently reformulated as a total distance

minimization problem, which can be expressed as

$$(\text{P3.2}): \min_{z_u,h} \sum_{k=1}^{K} [(x_k - x_u)^2 + (y_k - y_u)^2 + h^2] \tag{29}$$

$$\text{s.t. } \|z_k - z_u\|^2 \leq h^2 \tan^2 \Theta, \tag{30}$$

$$h_{min} \leq h \leq h_{max}, \tag{31}$$

$$\min\{x_i\} \leq x_u \leq \max\{x_i\}, 1 \leq i \leq K, \tag{32}$$

$$\min\{y_i\} \leq y_u \leq \max\{y_i\}, 1 \leq i \leq K. \tag{33}$$

It can be seen from problem (P3.2) that as the flight altitude h increases, so does the distance d_k between the UAV and device k. Therefore, to minimize the total path-loss between the UAV and devices, the optimal flight altitude h^* should be as small as possible within the range of the minimum threshold h_{min}, which can be achieved based on constraint (30)-(31) and is given by

$$h^* = \max\left\{\frac{\sqrt{D_{\max}}}{\tan\Theta}, h_{min}\right\}, \tag{34}$$

where $D_{\max} = \max_{k=1,\cdots,K} \|z_k - z_u\|^2$ represents the largest horizontal distance between the UAV and the devices. With h^* as given in (34), it can be shown that constraint (30) and (31) are satisfied and thus can be removed; furthermore, we can rewrite problem (P3.2) as

$$(\text{P3.3}): \min_{x_u,y_u} \sum_{k=1}^{K} [(x_k - x_u)^2 + (y_k - y_u)^2] \tag{35}$$

$$\text{s.t. } \min\{x_i\} \leq x_u \leq \max\{x_i\}, 1 \leq i \leq K, \tag{36}$$

$$\min\{y_i\} \leq y_u \leq \max\{y_i\}, 1 \leq i \leq K. \tag{37}$$

Problem (P3.3) is a convex optimization problem because its objective function is a convex function of (x_u, y_u) and all of its constraints specify a convex set of (x_u, y_u). Therefore, this problem can be effectively solved by using the first-order derivatives of x_u and y_u, and x_u^* and

y_u^* can be expressed as

$$x_u^* = \frac{\sum_{k=1}^{K} x_k}{K}, \quad y_u^* = \frac{\sum_{k=1}^{K} y_k}{K}. \tag{38}$$

After obtaining the 3D placement of the UAV, we employ a branch and bound algorithm [23], [25] to design the flight trajectory that minimizes the total flight distance. Next, we design the beam patterns of the antenna array by using the MOEA/D based algorithm.

B. Optimal phased array pattern

Based on the optimal 3D placement of the UAV (x_u^*, y_u^*, h^*) and the fixed transmit power p_k, it can be verified that all the constraints are satisfied, and the problem (P1) can be formulated as

$$(\mathrm{P4}): \max_{\mathbf{E}(\theta,\phi)} \sum_{k=1}^{K} \log_2(1 + SINR_k). \tag{39}$$

From (3), it is observed that the effective channel gain $|\mathbf{h}_k^H \mathbf{w}|^2$ increases with the increasing of the beamforming gain $|\mathbf{E}(\theta, \phi)|^2$. Consequently, the effective channel gain $|\mathbf{h}_k^H \mathbf{w}|^2$ increases, resulting in a significantly enhanced of the quality of UAV-ground communications, and therefore improves the achievable rates in UAV-aided mmWave MIMO-NOMA networks. To generate a steerable beam pattern, the key idea is to adjust the side-lobe level (SLL), array gain and beamwidth. This practice is usually referred to as the beam pattern synthesis of antenna arrays. Thus, problem (P4) can be converted into a beam pattern synthesis problem as

$$(\mathrm{P4.1}): \max \sum_{k=1}^{K} \mathbf{E}_k(\theta, \phi), \tag{40}$$

where $\mathbf{E}_k(\theta, \phi)$ represents the beam pattern of the antenna array steering to the device k. To solve the beam pattern synthesis problem, the phases of an $M \times N$ antenna array should be optimized, which can be formulated as a multiobjective optimization problem. Mathematically, the multiobjective optimization problem can be constructed as

$$\min \ F(\boldsymbol{\beta}) = (f_1(\boldsymbol{\beta}), f_2(\boldsymbol{\beta}), f_3(\boldsymbol{\beta}))^T \tag{41}$$

$$\text{s.t. } \boldsymbol{\beta} \in \mathbf{R}^{M\times N}, \tag{42}$$

where $f_1(\boldsymbol{\beta}) = SLL(\boldsymbol{\beta})$, $f_2(\boldsymbol{\beta}) = \frac{1}{|\mathbf{E}(\theta,\phi)|}$, $f_3(\boldsymbol{\beta}) = \frac{1}{|\Theta_{h,e}|}$ and $\boldsymbol{\beta} = [\beta_{1n}, \cdots, \beta_{mn}, \cdots, \beta_{MN}]^T$. $SLL(\boldsymbol{\beta}) = 20\log\frac{|AF_{msl}|}{|AF_{max}|}$ is the SLL of the $M\times N$ antenna array, where AF_{msl} and AF_{max} are the array factor of the maximum SLL and the array factor of main-lobe peak intensity, respectively. $\Theta_{h,e}$ denotes the elevation plane half-power beamwidth. Problem (41)-(42) is formulated to design beam patterns of the $M \times N$ antenna array by reducing the SLL, increasing the array gain and controlling the beamwidth. To solve this problem, we propose a MOEA/D based algorithm that has the following components:

- *Input*: The input parameters of the MOEA/D based algorithm are $\{iter, N_{pop}, \boldsymbol{\kappa}^i, T_{nei}\}$. Here, $iter$ denotes the number of iterations, N_{pop} is the number of sub-problems in the MOEA/D based algorithm. $\boldsymbol{\kappa}^i (i = 1, \cdots, N_{pop})$ indicates the weight vectors and T_{nei} is the number of weight vectors considered to be neighbors of each weight vector.
- *Output*: The output of the algorithm is a non-dominated set EP.
- *Initiation*: We first set EP=$\emptyset$. For each $i = 1, \cdots, N_{pop}$, we calculate T_{nei} nearest neighbors of the weight vector $\boldsymbol{\kappa}^i$ by the Euclidean distance, whose indexes are contained in $\hbar(i) = \{i_1, \cdots, i_{T_{nei}}\}$. Then, we generate the initiate solutions $\boldsymbol{\beta}_1, \cdots, \boldsymbol{\beta}_{N_{pop}}$ randomly and set $FV_i = F(\boldsymbol{\beta}_i)$, $\mathbf{z} = (z_1, \cdots, z_j, \cdots, z_d)^T$. Here, FV_i denotes the F-value of $\boldsymbol{\beta}_i$, and $z_j = \min\{f_j(\boldsymbol{\beta}), \boldsymbol{\beta} \in \mathbf{R}^{M\times N}\}$ is the best-so-far value for the objection function $f_j(\boldsymbol{\beta})$.
- *Update*: For each $i = 1, \cdots, N_{pop}$, we randomly select two indexes k, l from $\hbar(i)$, and then generate a new solution $\boldsymbol{y}$ from $\boldsymbol{\beta}_k$ and $\boldsymbol{\beta}_l$ by using the differential evolution (DE) method [26]. Subsequently, we update the best-so-far solutions and current solutions. Specifically, for each $j = 1, \cdots, d$, we set $z_j = f_j(\boldsymbol{y})$ if $z_j > f_j(\boldsymbol{y})$; for each $j \in \hbar(i)$, if $g^{te}(\boldsymbol{y} \mid \boldsymbol{\kappa}^j, \mathbf{z}) \leq g^{te}(\boldsymbol{\beta}_j \mid \boldsymbol{\kappa}^j, \mathbf{z})$, we set $\boldsymbol{\beta}_j = \boldsymbol{y}$ and $FV_j = F(\boldsymbol{y})$. Here, $g^{te}(\boldsymbol{y} \mid \boldsymbol{\kappa}^j, \mathbf{z}) = \max_{1\leq t\leq d}\{\kappa_t^j | f_t(\boldsymbol{y}) - z_t|\}$ [27]. In addition, $F(\boldsymbol{y})$ will be added to EP if it is not dominated by other vectors,

and all vectors from EP dominated by $F(\boldsymbol{y})$ are removed.

- *Stopping*: The algorithm will stop and output EP after $iter$ iterations; otherwise, go to *Update*.

The Pareto optimal solutions can be achieved by using the proposed MOEA/D based algorithm, which is given as follows.

Proposition 1: The Pareto optimal solutions of the multiobjective optimization problem are given by

$$EP^* = \{\boldsymbol{\beta}^*\} \tag{43}$$

$$= \{\boldsymbol{\beta} \in \mathbf{R}^{M\times N} | \neg \exists \boldsymbol{\beta}' \in \mathbf{R}^{M\times N}, f_i(\boldsymbol{\beta}') \leq f_i(\boldsymbol{\beta}^*)\},$$

$$i \in \{1, \cdots, 3\}. \tag{44}$$

Proof: Since the convergence performance of the MOEA/D based algorithm is similar in [23], [27], the proof of Proposition 1 is omitted here. ■

C. Power allocation schemes

1) Optimal power allocation: For the fixed 3D placement of the UAV (x_u^*, y_u^*, h^*) and beam pattern $\mathbf{E}_k^*(\theta, \phi)$, problem (P1) can be written as

$$(\text{P5}): \max_{p_k} \sum_{k=1}^{K} R_k \tag{45}$$

$$\text{s.t. } R_k \geq r_k, \tag{46}$$

$$\sum_{k=1}^{K} p_k \leq P_{max}. \tag{47}$$

It is obvious that problem (P5) is non-convex due to the non-convexity of the objective function and constraint (46). After the MOEA/D based algorithm for adaptive beamforming, the effective

channel power gain can be determined. In particular, for the convenience of later analysis in this paper, we set $|\mathbf{h}_1^H\mathbf{w}|^2 < |\mathbf{h}_2^H\mathbf{w}|^2 < \cdots < |\mathbf{h}_K^H\mathbf{w}|^2$ by selecting the proper value of phases from the Pareto set. Thus, from (6) and (7), problem (P5) can be reformulated as follows

$$(\mathrm{P}5.1): \max_{p_k} \sum_{k=1}^{K} \log_2\left(1+\frac{p_k|\mathbf{h}_k^H\mathbf{w}|^2}{\sum_{i=k+1}^{K} p_i|\mathbf{h}_k^H\mathbf{w}|^2+\sigma^2}\right) \tag{48}$$

$$\text{s.t. } R_k \geq r_k, \tag{49}$$

$$\sum_{k=1}^{K} p_k \leq P_{max}. \tag{50}$$

Problem (P5.1) is still a non-convex problem. One obstacle in solving problem (P5.1) is constraint (49). To overcome this problem, we transform the inequality (49) by using a logarithmic transformation as below

$$p_k \geq (2^{r_k}-1)\left(\sum_{i=k+1}^{K} p_i + \frac{\sigma^2}{|\mathbf{h}_k^H\mathbf{w}|^2}\right). \tag{51}$$

From (51), it is a linear function with respect to p_k, and thus is convex. In addition, according to [19], the objective function of problem (P5.1) can be reformulated as

$$\begin{aligned}\sum_{k=1}^{K} R_k = &\sum_{k=1}^{K-1} \log_2\left(\frac{\sum_{i=k+1}^{K} p_i|\mathbf{h}_{k+1}^H\mathbf{w}|^2+\sigma^2}{\sum_{i=k+1}^{K} p_i|\mathbf{h}_k^H\mathbf{w}|^2+\sigma^2}\right)\\ &+\log_2\left(1+\frac{P_{max}|\mathbf{h}_1^H\mathbf{w}|^2}{\sigma^2}\right).\end{aligned} \tag{52}$$

Thus, by substituting (51)-(52) into problem (P5.1), problem (P5.1) is equivalently expressed as

$$\begin{aligned}(\mathrm{P}5.2): \max_{p_k} &\sum_{k=1}^{K-1} \log_2\left(\frac{\sum_{i=k+1}^{K} p_i|\mathbf{h}_{k+1}^H\mathbf{w}|^2+\sigma^2}{\sum_{i=k+1}^{K} p_i|\mathbf{h}_k^H\mathbf{w}|^2+\sigma^2}\right)\\ &+\log_2\left(1+\frac{P_{max}|\mathbf{h}_1^H\mathbf{w}|^2}{\sigma^2}\right)\end{aligned} \tag{53}$$

$$\text{s.t. } p_k \geq (2^{r_k}-1)\left(\sum_{i=k+1}^{K} p_i + \frac{\sigma^2}{|\mathbf{h}_k^H\mathbf{w}|^2}\right), \tag{54}$$

$$\sum_{k=1}^{K} p_k \leq P_{max}. \tag{55}$$

The objective function of problem (P5.2) consists $(K-1)$ non-convex sub-functions. By discarding the constant term $\log_2\left(1+\frac{P_{max}|\mathbf{h}_1^H\mathbf{w}|^2}{\sigma^2}\right)$, the corresponding problem, for $k=1,2,\cdots,K-1$, can be converted into a sum-rate maximization problem. Therefore, with $b_k=\sum_{i=k+1}^{K} p_i$ and $U(b_k)=\log_2(b_k\cdot|\mathbf{h}_{k+1}^H\mathbf{w}|^2+\sigma^2)-\log_2(b_k\cdot|\mathbf{h}_k^H\mathbf{w}|^2+\sigma^2)$, $k=1,2,\cdots,K-1$, problem (P5.2) is reformulated as

$$(\text{P5.3}): \max_{p_k} \ \sum_{k=1}^{K-1} U(b_k) \tag{56}$$

$$\text{s.t. } p_k \geq (2^{r_k}-1)\left(\sum_{i=k+1}^{K} p_i + \frac{\sigma^2}{|\mathbf{h}_k^H\mathbf{w}|^2}\right), \tag{57}$$

$$\sum_{k=1}^{K} p_k \leq P_{max}. \tag{58}$$

Although problem (P5.3) is still not convex due to the non-convexity of its objective function, it can be transformed into a convex optimization problem through the monotonicity property. Specifically, the first-order derivative of $U(b_k)$ can be expressed as

$$\frac{\partial U(b_k)}{\partial b_k}=\frac{1}{\ln 2}\left[\frac{(|\mathbf{h}_{k+1}^H\mathbf{w}|^2-|\mathbf{h}_k^H\mathbf{w}|^2)\sigma^2}{(b_k\cdot|\mathbf{h}_{k+1}^H\mathbf{w}|^2+\sigma^2)(b_k\cdot|\mathbf{h}_k^H\mathbf{w}|^2+\sigma^2)}\right]. \tag{59}$$

Consider the decoding order and because $|\mathbf{h}_{k+1}^H\mathbf{w}|^2>|\mathbf{h}_k^H\mathbf{w}|^2$, it follows that $\frac{\partial U(b_k)}{\partial b_k}>0$. As a result, by substituting (59) into problem (P5.3), problem (P5.3) can be equivalently expressed as

$$(\text{P5.4}): \max_{p_k} \ b_s \tag{60}$$

$$\text{s.t. } p_k \geq (2^{r_k}-1)\left(\sum_{i=k+1}^{K} p_i + \frac{\sigma^2}{|\mathbf{h}_k^H\mathbf{w}|^2}\right), \tag{61}$$

$$\sum_{k=1}^{K} p_k \leq P_{max}, \tag{62}$$

$$1 \leq k \leq K, \tag{63}$$

$$1 \leq s \leq K-1. \tag{64}$$

Given the convexity of problem (P5.4), the optimal solution can be obtained by using standard convex optimization techniques. In the following, the Karush-Kuhn-Tucker (KKT) conditions [28] is applied to achieve the closed-form expressions of transmit power. Thus, let ν and μ_k be the Lagrange multipliers. Associate the Lagrange multiplier ν with the transmit power constraint, and μ_k with the minimum rate constraints, the KKT conditions are then

$$\nu = \begin{cases} \mu_k - \sum_{i=1}^{k-1} \mu_i (2^{r_k} - 1), & 1 \leq k \leq s, \\ \mu_k - \sum_{i=1}^{k-1} \mu_i (2^{r_k} - 1) + 1, & s+1 \leq k \leq K, \end{cases} \tag{65}$$

$$\mu_k \left[(2^{r_k} - 1) \left(\sum_{i=k+1}^{K} p_i + \frac{\sigma^2}{|\mathbf{h}_k^H \mathbf{w}|^2} \right) - p_k \right] = 0, \tag{66}$$

$$\mu_k \geq 0, \quad k = 1, 2, \cdots, K, \tag{67}$$

From (65)-(67), we can obtain the closed-form expressions for the transmit power of problem (P5) that are given in Proposition 2.

Proposition 2: The closed-form expressions of transmit power p_k can be obtained if and only if $\mu_k > 0$ holds, which can be expressed as

$$p_k^* = \begin{cases} \frac{(2^{r_k} - 1)\left(P_{max} - \sum_{i=1}^{k-1} p_i + \frac{\sigma^2}{|\mathbf{h}_k^H \mathbf{w}|^2} \right)}{2^{r_k}}, & 1 \leq k \leq K-1, \\ P_{max} - \sum_{i=1}^{K-1} p_i^*, & k = K. \end{cases} \tag{68}$$

Proof: First, consider the case of $\mu_k = 0$, from (65) and setting $k = 1$, it follows that $\nu = \mu_1 = 0$. For $1 \leq k \leq s$, from (65), it follows that $\mu_k = \sum_{i=1}^{k-1} \mu_i (2^{r_k} - 1)$. For $k = s+1$, we have $\mu_1 = \nu = \mu_{s+1} - \sum_{i=1}^{s} \mu_i (2^{r_k} - 1) + 1 = \mu_{s+1} + 1 > 0$, which contradicts to $\mu_1 = 0$. This

implies that $\mu_k \neq 0$. Next, consider the case of $\mu_k > 0$, setting $k = 1$, it follows $\nu = \mu_1 > 0$. For $1 \leq k \leq s$, it follows $\mu_k = \sum_{i=1}^{k-1} \mu_i(2^{r_k} - 1) + \nu$. Given the fact that $\nu > 0$, we have $\mu_k > 0$, $1 < k < s$. In this case, by substituting $\sum_{i=k+1}^{K} p_i$ in (66) with $(P_{max} - \sum_{i=1}^{k} p_i)$, $s = K - 1$, we have the closed-form expressions of the transmission power p_k^* as follows

$$p_k^* = \begin{cases} \dfrac{(2^{r_k}-1)\left(P_{max} - \sum_{i=1}^{k-1} p_i + \frac{\sigma^2}{|\mathbf{h}_k^H \mathbf{w}|^2}\right)}{2^{r_k}}, & 1 \leq k \leq K-1, \\ P_{max} - \sum_{i=1}^{K-1} p_i^*, & k = K. \end{cases} \tag{69}$$

This completes the proof of the Proposition 2. ■

2) Sub-optimal power allocation: The previous sub-section presents the optimal power allocation scheme to achieve the closed-form expressions of the transmit power; however, this scheme requires large-scale channel state information (CSI) in the network. Next, we propose an effective algorithm for transmit power allocation, which approximates the performance of the optimal power allocation scheme in a purely localized manner. In particular, we rewrite the problem (P5.1) as

$$(\text{P6}): \max_{p_k} \sum_{k=1}^{K} \log_2 \left(1 + \frac{p_k |\mathbf{h}_k^H \mathbf{w}|^2}{\sum_{i=k+1}^{K} p_i |\mathbf{h}_k^H \mathbf{w}|^2 + \sigma^2}\right) \tag{70}$$

$$\text{s.t. } p_k \geq (2^{r_k} - 1)\left(\sum_{i=k+1}^{K} p_i + \frac{\sigma^2}{|\mathbf{h}_k^H \mathbf{w}|^2}\right), \tag{71}$$

$$\sum_{k=1}^{K} p_k \leq P_{max}. \tag{72}$$

It is observed that $p_k |\mathbf{h}_k^H \mathbf{w}|^2$ and $\sum_{i=k+1}^{K} p_i |\mathbf{h}_k^H \mathbf{w}|^2 + \sigma^2$ of problem (P6) are all positive functions, and the objective function is a number of scale nondecreasing functions. Therefore, to facilitate the solution, we transform the objective function using the following lemma.

Lemma 3.1 ([29]): For $m = 1, 2, \cdots, M$, given the nondecreasing functions $f_m(\cdot)$, $A_m(\mathbf{x})$:

$\mathbf{R}^d \to \mathbf{R}_+$ and $B_m(\mathbf{x}) : \mathbf{R}^d \to \mathbf{R}_{++}$, the sum-of-functions-of-ratio problem

$$\max_{\mathbf{x}} \sum_{m=1}^{M} f_m\left(\frac{A_m(\mathbf{x})}{B_m(\mathbf{x})}\right) \tag{73}$$

$$\text{s.t. } \mathbf{x} \in \mathcal{X}, \mathcal{X} \subseteq \mathbf{R}^d \tag{74}$$

can be equivalently expressed as a convex optimization problem if and only if this problem satisfies the following conditions.

Let the function $\frac{A_m(\mathbf{x})}{B_m(\mathbf{x})}$, $m = 1, 2, \cdots, M$, have the form $g(\mathbf{x}, y_m) = t(A_m(\mathbf{x}))q_1(y_m) + h(B_m(\mathbf{x}))q_2(y_m)$. Then, $y_m^* = \text{argmax}_{y_m} g(\mathbf{x}, y_m)$ and $g(\mathbf{x}, y_m^*) = A_m(\mathbf{x})/B_m(\mathbf{x})$ can achieve the same solution $\mathbf{x}$, where $t(\cdot)$, $q_1(\cdot)$, $h(\cdot)$ and $q_2(\cdot)$ are all functions.

Thus, the equivalent problem is given as

$$\max_{\mathbf{x},\mathbf{y}} \sum_{m=1}^{M} f_m\left(2y_m\sqrt{A_m(\mathbf{x})} - y_m^2 B_m(\mathbf{x})\right) \tag{75}$$

$$\text{s.t. } \mathbf{x} \in \mathcal{X}, \mathcal{X} \subseteq \mathbf{R}^d, \tag{76}$$

$$y_m \subseteq \mathbf{R}, m = 1, 2, \cdots, M, \tag{77}$$

where $\mathbf{y} = \{y_1, \cdots, y_m, \cdots, y_M\}$, $y_m = \frac{\sqrt{A_m(\mathbf{x})}}{B_m(\mathbf{x})}$ is an auxiliary variable, and the transformed problem is convex with the y_m.

Since problem (P6) satisfies the conditions of Lemma 3.1, we can apply Lemma 3.1 to transform the objective function into a convex function. In particular, let $A_k(p_k) = p_k|\mathbf{h}_k^H\mathbf{w}|^2$, $B_k(p_k) = \sum_{i=k+1}^{K} p_i|\mathbf{h}_k^H\mathbf{w}|^2 + \sigma^2$, $C_k = A_k(p_k)/B_k(p_k)$. Consider the equivalent problem in (75)-(77), C_k can be replaced with $(2y_k\sqrt{A_k(p_k)} - y_k^2 B_k(p_k))$, and thus problem (P6) is equivalently written as

$$(\text{P6.1}) : \max_{p_k, y_k} \sum_{k=1}^{K} G_k \tag{78}$$

$$\text{s.t. } p_k \geq (2^{r_k}-1)\left(\sum_{i=k+1}^{K} p_i + \frac{\sigma^2}{|\mathbf{h}_k^H\mathbf{w}|^2}\right), \tag{79}$$

$$\sum_{k=1}^{K} p_k \leq P_{max}, \tag{80}$$

where

$$G_k = \log_2\left(1+2y_k\sqrt{p_k|\mathbf{h}_k^H\mathbf{w}|^2} - y_k^2\left(\sum_{i=k+1}^{K} p_i|\mathbf{h}_k^H\mathbf{w}|^2+\sigma^2\right)\right), \tag{81}$$

$$y_k = \frac{\sqrt{A_k(p_k)}}{B_k(p_k)} = \frac{\sqrt{p_k|\mathbf{h}_k^H\mathbf{w}|^2}}{\sum_{i=k+1}^{K} p_i|\mathbf{h}_k^H\mathbf{w}|^2+\sigma^2}. \tag{82}$$

Problem (P6.1) is a convex optimization problem with fixed y_k, Therefore, we propose a FP-based suboptimal algorithm to tackle this problem effectively whose procedure is summarized in TABLE I. The suboptimal algorithm works as follows. In each step, y_k is first updated by using (82). Then, the value of function G_k is maximized over p_k, while keeping y_k's fixed. Since G_k is nondecreasing with each iteration, the proposed algorithm can converge to a stationary point, whose convergence performance is analyzed as the following proposition.

Proposition 3: The FP-based suboptimal algorithm optimizes y_k and p_k in an iterative manner, and converges to a stationary point with the optimal y_k^* that is given as

$$y_k^* = \frac{\sqrt{p_k|\mathbf{h}_k^H\mathbf{w}|^2}}{\sum_{i=k+1}^{K} p_i|\mathbf{h}_k^H\mathbf{w}|^2+\sigma^2}. \tag{83}$$

Proof: As mentioned earlier, problem (P6.1) is a convex optimization problem with fixed y_k that updates its value by using (82), and thus the FP-based suboptimal algorithm can obtain a fixed point p_k at each iteration. Since the proposed algorithm is the block coordinate ascent algorithm [29], it can converge to a stationary point based on the optimal y_k^* by using the equation (83). On the other hand, from Lemma 3.1, problem (P6) is equivalent to the problem (P6.1) due to the equivalence in the solution and the equivalence in the objection function. However, due to the non-convexity of problem (P6), the proposed algorithm can only converge to a local optimum

TABLE I: THE FP-BASED SUBOPTIMAL ALGORITHM

1) **INITIALIZE:**
Initiation p_k to a feasible point;
Replace $A_k(p_k)/B_k(p_k)$ of problem (P6)
with $2y_k\sqrt{A_k(p_k)} - y_k^2 B_k(p_k)$;
2) **REPEAT**
3) Update y_k by (82);
4) Update p_k by solving the convex problem (P6.1),
over p_k for fixed y_k.
5) **Until:** The value of function G_k in (81) converges.

[29]. Therefore, this completes the proof of Proposition 3. ■

IV. Simulation results

In this section, numerical results are provided to validate the performance of our proposed algorithms in UAV-aided mmWave MIMO-NOMA networks. To study the sum-rate performance, we adopt a mmWave channel used in [22], [30] with a carrier frequency at 25 GHz. The noise power σ^2 is set to -110 dBm, and the mean square additional loss is assumed to be $\eta_{LoS} = 0.1$ dB. The path loss factor α is set to 2 [31]. It is assumed that $K = 12$ IoT devices are randomly distributed in a 500×500 m^2 square area, and all devices are divided into $\Gamma = 4$ groups. The maximum effective illumination 2Θ is set to 80°, and the amplitude and spacing of the antenna array are 1 A and 5.5 mm, respectively. The maximum transmit power of the UAV P_{max} and the minimum rate constraint of devices r_k are set to 80 mW and 1 bit/s/Hz, respectively. To take into account UAV regulations, the minimum altitude h_{min} and maximum altitude h_{max} are set to 21 m and 120 m [21], respectively.

In the first simulation, the convergence behavior of the FP-based suboptimal algorithm is evaluated by illustrating how the sum rate behaves with the number of iterations. It can be seen in Fig. 2 that the proposed algorithm can converge to a stable value, and the point of initiation $P^{(0)}$ affects the convergence speed of the algorithm. In particular, the sum rate converges to a

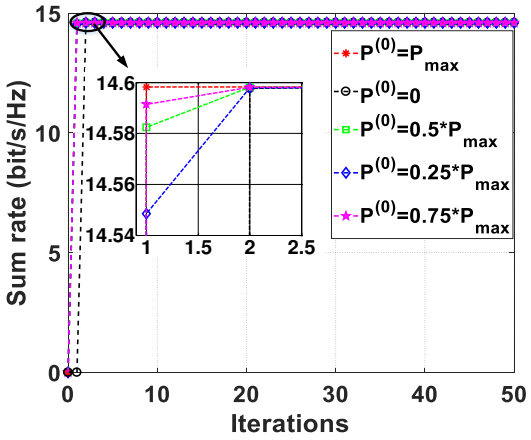

Fig. 2: An example of convergence behavior of the FP-based suboptimal algorithm in terms of sum rate.

fixed value after approximately two iterations when $P^{(0)} = 0$, $0.5P_{max}$, $0.25P_{max}$, $0.75P_{max}$, but the iterative number is reduced to one when $P^{(0)} = P_{max}$ is chosen. This result demonstrates that the proposed algorithm converges to a stable point nearly within two iterations.

In the next simulation, the beam pattern synthesis of an antenna array by using the MOEA/D based algorithm are evaluated and presented in Fig. 3. The 8×8 antenna array is separated into four sub-arrays, wherein the size of each sub-array is 4×4. As shown in Fig. 3(a), four beams formed by the antenna array are steered to four devices, whose directions are $(-30°, 90°)$, $(-10°, 90°)$, $(0°, 90°)$ and $(20°, 90°)$, respectively. The main beam gains for all beams are 10 dB greater than the first sidelobe levels. Furthermore, the beam pattern synthesis achieved by the MOEA/D based algorithm in MATLAB is very close to the high frequency structure simulator (HFSS). This is because that the MOEA/D based algorithm aims to optimize the phases of the antenna array by considering the mutual coupling between antenna elements within each sub-array, and hence the simulation results obtained by the MOEA/D based algorithm in MATLAB match those by HFSS. Accordingly, the non-dominated set of the above four beam directions found by the MOEA/D based algorithm for three hundred iterations is shown in Fig. 3(b). It can be seen that most of the non-dominated solutions of each beam direction lie on a real Pareto front. This is due to the fact that a new non-dominated solution set is close to the Pareto-optimal solutions

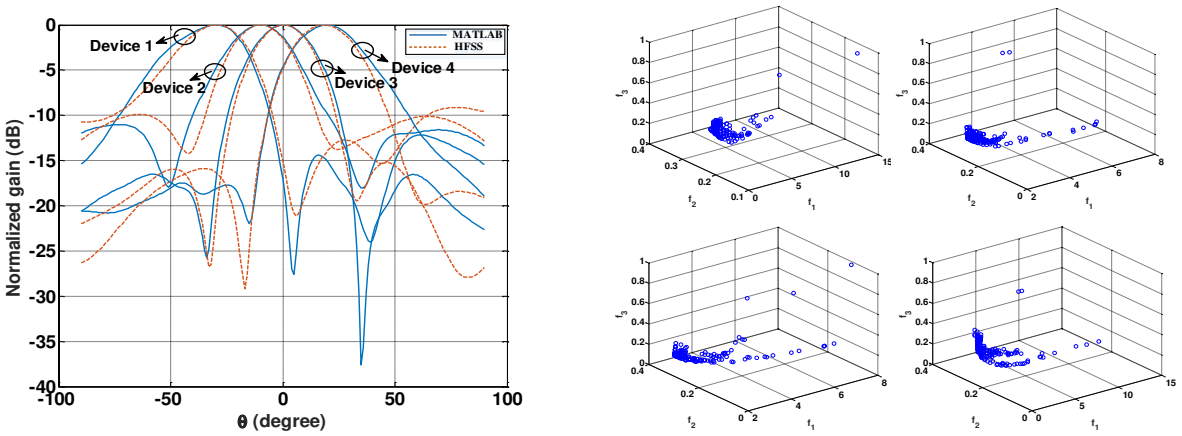

(a) (b)

Fig. 3: Multi-beam gain performance for a UAV-aided mmWave MIMO-NOMA system with the MOEA/D based algorithm: (a) Illustration of a UAV-aided mmWave MIMO-NOMA system with multi-beams generated by an 8×8 uniform planner array (UPA); (b) An example of convergence behavior of the MOEA/D based algorithm for 3-objective optimization problem.

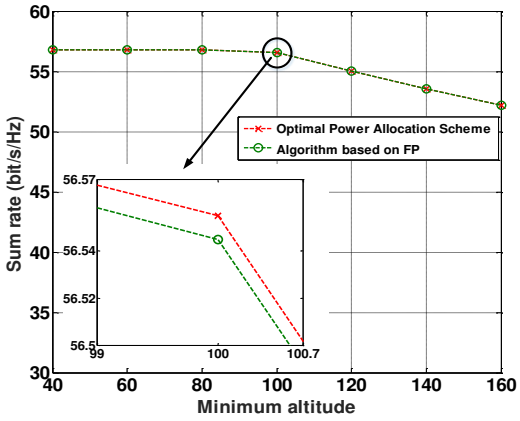

Fig. 4: The performance of two proposed power allocation schemes (sum rate versus the minimum altitude).

than the previous solution after each iteration, and thereby the algorithm can obtain the optimal solutions with infinite iterations. Moreover, it can be seen that different phases of the antenna array can achieve different array gain, SLL and beamwidth of the synthesized beam pattern. For example, a high-gain steerable beam pattern may also have practically high SLL and wide beamwidth. As a result, there is a trade-off between the array gain, SLL and beamwidth of the beam pattern.

Furthermore, the sum-rate performance of the proposed two power allocation schemes with

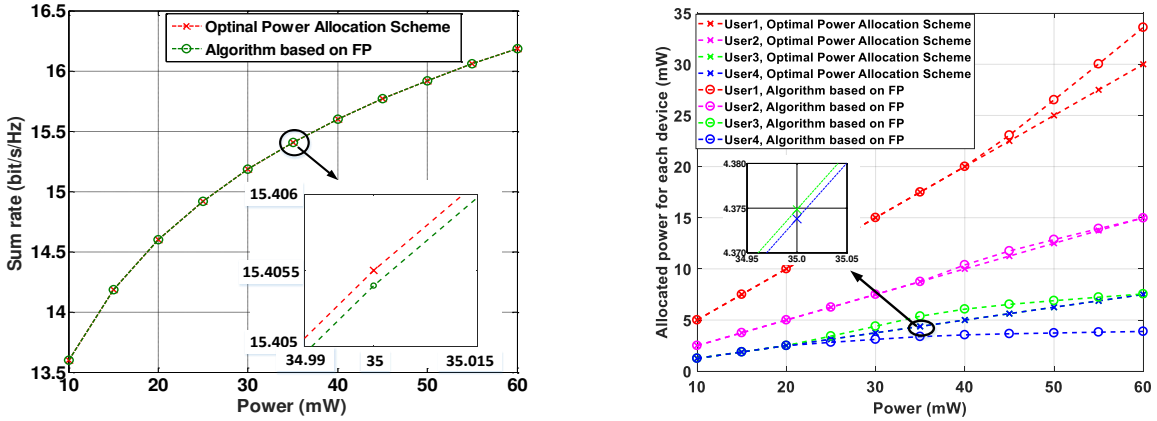

(a) (b)

Fig. 5: The performance of two proposed power allocation schemes: (a) Sum rate versus transmit power; (b) The allocated power for each device versus the maximum transmit power.

various QoS demands are evaluated in Fig. 4, Fig. 5 and Fig. 6. We first investigate the sum-rate performance of the two proposed solutions under different minimum altitude of the UAV. As shown in Fig. 4, the sum rate is the same up to a lower minimum altitude, i.e., $40 \leq h_{min} \leq 100$ m. This is due to the fact that the defined minimum altitude h_{min} is lower than the optimal altitude $\frac{\sqrt{D_{\max}}}{\tan\Theta}$, and hence the sum rate remains stable. When h_{min} exceeds 100 m, the sum rate decreases thereafter. In this case, $\frac{\sqrt{D_{\max}}}{\tan\Theta}$ is less than h_{min}, and thus the sum rate decreases according to (34). Next, we show the sum rate under different transmit power budget. As shown in Fig. 5(a), the sum rate increases dramatically with a lower power budget, i.e., $P_{max} < 35$ mW, and then approaches an asymptotic value for both schemes. This is due to the fact that increasing the transmit power for one user will increase the interference for other devices in the same NOMA group, and hence the sum rate of the system approaches an asymptotic value for high available transmit power at the UAV. Furthermore, the sum rate achieved by the FP-based suboptimal algorithm is very close to the optimal power allocation scheme. Besides, the allocated power for each device versus the maximum transmit power for the two proposed power allocation schemes are also investigated. It can be seen in Fig. 5(b) that the allocated power for devices increases monotonically as the maximum transmit power of the UAV increases. Moreover, for

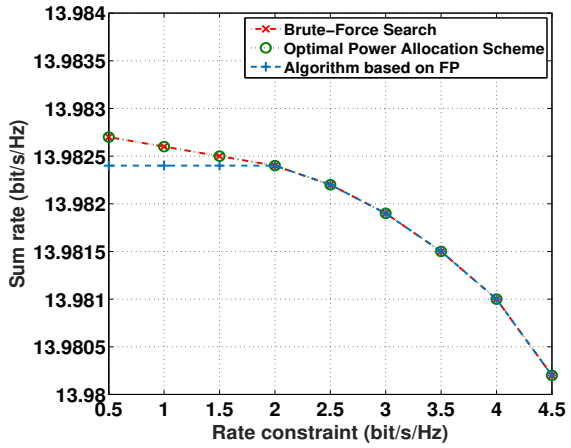

Fig. 6: The performance of two proposed power allocation schemes (sum rate versus rate constraint).

both power allocation schemes, it can be observed that the devices with poor channel quality are assigned more power than the devices with good channel quality. This is due to the fact that the weak users should be decoded first according to SIC, and hence the weak devices are allocated more transmit power to mitigate the interference from the strong devices. We also investigate the sum rate versus the minimum required data rate per user for the two proposed schemes. As shown in Fig. 6, the sum rate decreases slowly in the lower rate constraint region, i.e., $0.5 \leq r_k < 2$ bit/s/Hz, and then decreases rapidly when $r_k > 2$ bit/s/Hz. This is due to the fact that satisfying a lower rate constraint consumes smaller transmit power, and hence the remaining transmit power can be allocated to achieve the optimal sum rate. On the contrary, when r_k is high, more power should be assigned to satisfy the minimum data rate requirement of the devices, and therefore less transmit power can be assigned to boost the sum rate. Thus, the curves decrease rapidly when $r_k > 2$. Furthermore, the sum rate achieved by the optimal power allocation scheme is the same as the Brute-Force search approach.

We then evaluate the performance of the trajectory design on the horizontal plane for a UAV-aided mmWave MIMO-NOMA system with $K = 12$ devices. As shown in Fig. 7, it can be observed that the locations of the UAV tend to lie in the center of devices in the same group. This can be attributed to the fact that the positions of the UAV locating at the middle of all devices

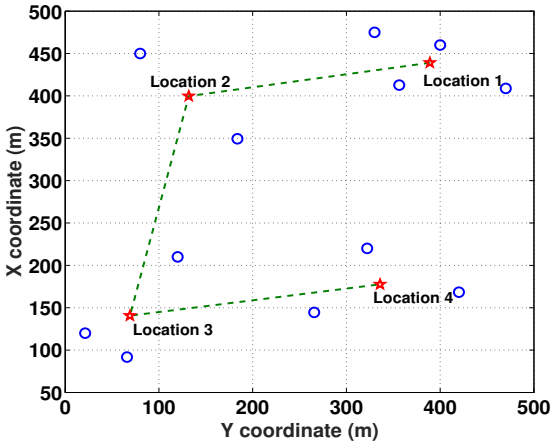

Fig. 7: Trajectory design for a UAV-aided mmWave MIMO-NOMA system with $K = 12$ devices.

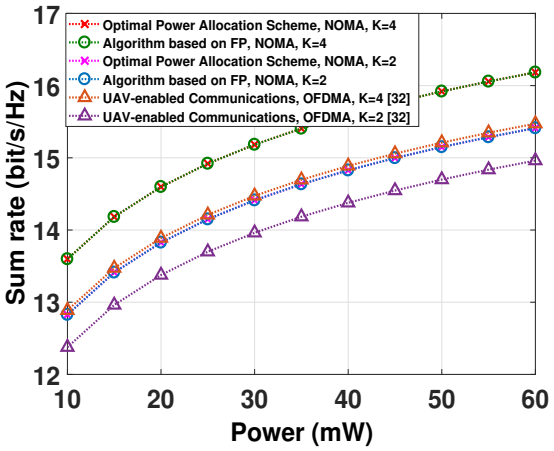

Fig. 8: Impact of the maximum transmit power on the sum rate performance under different resource allocation approaches.

in the same serving area can minimize the path-loss of UAV-ground transmission according to (38), such that the total rate of all devices can be maximized. However, this leads to a near-far problem; that is, the devices with good channel quality can achieve high data rate, and hence how to ensure the fairness among all devices is an open question and will become our future research work. Besides, it can be seen that the proposed trajectory scheme can minimize the flight distance to visit all the hover locations, and thus save the energy consumption.

Finally, we show the sum rate for both optimal and suboptimal power allocation, and compares them to the OFDMA scheme, for which equal power is allocated to all antenna elements. In order

to validate the effectiveness of our proposed schemes, we apply the iterative algorithm in a UAV-enabled OFDMA system [32] for comparison. In the UAV-enabled OFDMA system, a number of resource blocks are allocated to users, where each block is occupied exclusively. As shown in Fig. 8, the sum rate achieved by all the approaches are monotonically increasing with the maximum transmit power, but has a decreasing gain as the maximum transmit power increases (similar to the results in Fig. 5). In addition, the sum rates achieved by our two proposed schemes outperform the OFDMA scheme. This is due to the fact that the OFDMA scheme allocates each frequency resource to one user. To satisfy the QoS requirement of users, the UAV should utilize large transmit power to meet the minimum rate requirements of users, resulting in less transmit power that can be assigned to users, and thus restrict the improvement of sum rate. On the other hand, our proposed schemes employ NOMA which enables multiple users to utilize the same bandwidth resource, resulting in full exploitation of multi-user diversity in the power domain, and thereby achieves a higher spectral efficiency. Therefore, it is demonstrated that our proposed joint 3D deployment, beam pattern design and power allocation algorithm can significantly improve the system performance in terms of sum rate for all IoT devices.

V. Conclusion

In this paper, we study a UAV-aided mmWave MIMO-NOMA system, in which a UAV acts as a flying BS and supports massive IoT devices connections. Aiming to maximize the sum rate of all IoT devices, we formulate a sum-rate maximization problem subject to the minimum rate requirement of IoT devices, coverage radius and transmit power of the UAV. Due to the intractability and non-convexity of this problem, we propose a joint 3D deployment, beam pattern design and power allocation algorithm to decompose the optimization problem into three sub-problems, and optimize the 3D placement of the UAV, beam pattern and transmit power sequentially. Numerical results illustrate that the sum rate performance of all IoT devices can be significantly improved by the proposed algorithm compared to the OFDMA scheme.

REFERENCES

[1] W. Feng, J. Tang, Y. Yu, J. Song, N. Zhao, G. Chen, K.-K. Wong, and J. Chambers, "UAV-enabled SWIPT in IoT networks for emergency communications," *IEEE Wireless Commun.*, to be published, DOI: 10.1109/MWC.001.1900656.

[2] Z. Xiao, L. Zhu, J. Choi, P. Xia, and X. Xia, "Joint power allocation and beamforming for non-orthogonal multiple access (NOMA) in 5G millimeter wave communications," *IEEE Trans. Wireless Commun.*, vol. 17, no. 5, pp. 2961–2974, May 2018.

[3] J. Tang, D. K. C. So, A. Shojaeifard, K. Wong, and J. Wen, "Joint antenna selection and spatial switching for energy efficient MIMO SWIPT system," *IEEE Trans. Wireless Commun.*, vol. 16, no. 7, pp. 4754–4769, Jul. 2017.

[4] J. Tang, D. K. C. So, N. Zhao, A. Shojaeifard, and K. Wong, "Energy efficiency optimization with SWIPT in MIMO broadcast channels for Internet of Things," *IEEE Internet Things J.*, vol. 5, no. 4, pp. 2605–2619, Aug. 2018.

[5] Z. Ding, X. Lei, G.K. Karagiannidis, R. Schober, J. Yuan, and V.K. Bhargava, "A survey on non-orthogonal multiple access for 5G networks: Research challenges and future trends," *IEEE J. Sel. Areas Commun.*, vol. 35, no. 10, pp. 2181–2195, Oct. 2017.

[6] F. Fang, H. Zhang, J. Cheng, and V.C.M. Leung, "Energy-efficient resource allocation for downlink non-orthogonal multiple access network," *IEEE Trans. Commun.*, vol. 64, no. 9, pp. 3722–3732, Sep. 2016.

[7] Y. Zhang, H. Wang, Q. Yang, and Z. Ding, "Secrecy sum rate maximization in non-orthogonal multiple access," *IEEE Commun. Lett.*, vol. 20, no. 5, pp. 930–933, May 2016.

[8] D. Zhai, R. Zhang, L. Cai, B. Li, and Y. Jiang, "Energy-efficient user scheduling and power allocation for NOMA-based wireless networks with massive IoT devices," *IEEE Internet Things J.*, vol. 5, no. 3, pp. 1857–1868, Jun. 2018.

[9] H. Zhang, B. Wang, C. Jiang, K. Long, A. Nallanathan, V.C.M. Leung, and H.V. Poor, "Energy efficient dynamic resource optimization in NOMA system," *IEEE Trans. Wireless Commun.*, vol. 17, no. 9, pp. 5671–5683, Sep. 2018.

[10] D. Zhang, Z. Zhou, C. Xu, Y. Zhang, J. Rodriguez, and T. Sato, "Capacity analysis of NOMA with mmWave massive MIMO systems," *IEEE J. Sel. Areas Commun.*, vol. 35, no. 7, pp. 1606–1618, Jul. 2017.

[11] Z. Xiao, L. Zhu, Z. Gao, D.O. Wu, and X. Xia, "User fairness non-orthogonal multiple access (NOMA) for millimeter-wave communications with analog beamforming," *IEEE Trans. Wireless Commun.*, vol. 18, no. 7, pp. 3411–3423, Jul. 2019.

[12] Z. Wei, L. Zhao, J. Guo, D.W.K. Ng, and J. Yuan, "Multi-beam NOMA for hybrid mmwave systems," *IEEE Trans. Commun.*, vol. 67, no. 2, pp. 1705–1719, Feb. 2019.

[13] J. Xu, Y. Zeng, and R. Zhang, "UAV-enabled wireless power transfer: Trajectory design and energy optimization," *IEEE Trans. Wireless Commun.*, vol. 17, no. 8, pp. 5092–5106, Aug. 2018.

[14] L. Xie, J. Xu, and R. Zhang, "Throughput maximization for UAV-enabled wireless powered communication networks," *IEEE Internet Things J.*, vol. 6, no. 2, pp. 1690–1703, Apr. 2019.

[15] N. Zhao, W. Lu, M. Sheng, Y. Chen, J. Tang, F.R. Yu, and K.-K. Wong, "UAV-assisted emergency networks in disasters," *IEEE Wireless Commun.*, vol. 26, no. 1, pp. 45–51, Feb. 2019.

[16] J. Zhao, F. Gao, Q. Wu, S. Jin, Y. Wu, and W. Jia, "Beam tracking for UAV mounted SatCom on-the-move with massive antenna array," *IEEE J. Sel. Areas Commun.*, vol. 36, no. 2, pp. 363–375, Feb. 2018.

[17] Y. Sun, D. Xu, D.W.K. Ng, L. Dai, and R. Schober, "Optimal 3D-trajectory design and resource allocation for solar-powered UAV communication systems," *IEEE Trans. Commun.*, vol. 67, no. 6, pp. 4281–4298, Jun. 2019.

[18] Y. Liu, Z. Qin, Y. Cai, Y. Gao, G.Y. Li, and A. Nallanathan, "UAV communications based on non-orthogonal multiple access," *IEEE Wireless Commun.*, vol. 26, no. 1, pp. 52–57, Feb. 2019.

[19] X. Liu, J. Wang, N. Zhao, Y. Chen, S. Zhang, Z. Ding, and F.R. Yu, "Placement and power allocation for NOMA-UAV networks," *IEEE Wireless Commun. Lett.*, vol. 8, no. 3, pp. 965–968, Jun. 2019.

[20] T. Hou, Y. Liu, Z. Song, X. Sun, and Y. Chen, "Multiple antenna aided NOMA in UAV networks: A stochastic geometry approach," *IEEE Trans. Commun.*, vol. 67, no. 2, pp. 1031–1044, Feb. 2019.

[21] N. Rupasinghe, Y. Yapıcı, İ. Güvenç, and Y. Kakishima, "Non-orthogonal multiple access for mmWave drone networks with limited feedback," *IEEE Trans. Commun.*, vol. 67, no. 1, pp. 762–777, Jan. 2019.

[22] Y. Zeng, X. Xu, and R. Zhang, "Trajectory design for completion time minimization in UAV-enabled multicasting," *IEEE Trans. Wireless Commun.*, vol. 17, no. 4, pp. 2233–2246, Apr. 2018.

[23] W. Feng, N. Zhao, S. Ao, J. Tang, X. Zhang, Y. Fu, D.K.C. So, and K.-K. Wong, "Joint 3D trajectory design and time allocation for UAV-enabled wireless power transfer networks," *IEEE Trans. Veh. Technol.*, to be published, DOI: 10.1109/TVT.2020.2972133.

[24] C.A. Balanis, *Antenna Theory: Analysis and Design*. New York, NY, USA: Wiley, 2016.

[25] K.N. Singh and D.L. van Oudheusden, "A branch and bound algorithm for the traveling purchaser problem," *Eur. J. Oper. Res.*, vol. 97, no. 3, pp. 571–579, 1997.

[26] R. Storn and K. Price, "Differential evolution: A simple and efficient heuristic for global optimization over continuous spaces," *J. Global Optimization*, vol. 11, no. 4, pp. 341–359, Dec. 1997.

[27] Q. Zhang and H. Li, "MOEA/D: A multi-objective evolutionary algorithm based on decomposition," *IEEE Trans. Evol. Comput.*, vol. 11, no. 6, pp. 712–731, Dec. 2007.

[28] S. Boyd and L. Vandenberghe, *Convex Optimization*. Cambridge, U.K.: Cambridge Univ. Press, 2004.

[29] K. Shen and W. Yu, "Fractional programming for communication systems-Part I: Power control and beamforming," *IEEE Trans. Signal Process.*, vol. 66, no. 10, pp. 2616–2630, May 2018.

[30] L. Zhu, J. Zhang, Z. Xiao, X. Cao, D.O. Wu, and X. Xia, "3-D beamforming for flexible coverage in millimeter-wave UAV communications," *IEEE Wireless Commun. Lett.*, vol. 8, no. 3, pp. 837–840, Jun. 2019.

[31] Y. Zeng and R. Zhang, "Energy-efficient UAV communication with trajectory optimization," *IEEE Trans. Wireless Commun.*, vol. 16, no. 6, pp. 3747–3760, Jun. 2017.

[32] Z. Yang, C. Pan, M. Shikh-Bahaei, W. Xu, M. Chen, M. Elkashlan, and A. Nallanathan, "Joint altitude, beamwidth, location, and bandwidth optimization for UAV-enabled communications," *IEEE Commun. Lett.*, vol. 22, no. 8, pp. 1716–1719, Aug. 2018.